Chaos, Solitons and Fractals 165 (2022) 112808

Contents lists available at ScienceDirect

Chaos, Solitons and Fractals

journal homepage: www.elsevier.com/locate/chaos

Chimera states under genuine local coupling

Vladimir García-Morales [a,*], José A. Manzanares [a], Katharina Krischer [b]

[a] Departament de Física de la Terra i Termodinàmica, Universitat de València, Dr. Moliner, 50, E-46100 Burjassot, Spain
[b] Nonequilibrium Chemical Physics, Physics Department, Technische Universität München, James-Franck-Str. 1, D-85748 Garching, Germany

ARTICLE INFO

Keywords:
Nonlinear dynamics
Noise
Non-equilibrium and quantum processes

ABSTRACT

Chimera states, important forms of spatiotemporal self-organization in ensembles of identical oscillators, have been found in a wide variety of systems, provided that the coupling between the oscillators was nonlocal or global. Therefore, it is generally assumed that a locally coupled oscillatory medium, as described by the complex Ginzburg–Landau equation (CGLE), does not support chimera states. Here we show an alternative mechanism that does indeed lead to chimera states in a purely locally-coupled system, namely the interaction of an oscillatory medium, in the present case the CGLE, with a bistable internal degree of freedom.

1. Introduction

Chimera states in ensembles of identical nonlinear oscillators have been the subject of intense theoretical and experimental research (see [1–5] for excellent reviews). The term *chimera* was first coined in [6] in relation to previous results by Kuramoto and his coworkers [7,8]. In a chimera state, an ensemble of identical oscillators splits into two domains, one consisting of synchronous oscillators and the other of incoherent ones [6].

Chimeras have been associated with a variety of systems, ranging from biological and neuronal, to ecological and technological [9]. Initially, they were considered a peculiar coexistence of synchronized and desynchronized states, but after one decade chimera states turned out to be an important new paradigm of nonlinear dynamics at the interface of physical and life sciences [4]. Chimeras have been discussed to be related to uni-hemispheric sleep of aquatic mammals and migratory birds [10] and electrocorticographic recordings of epileptic seizures [11,12]. Chimera states have also been linked to power grid outages and optomechanics [4].

In the early work, a nonlocal spatial coupling of the oscillators was believed to be an essential feature for the occurrence of chimera states [6–8,13–17]. Meanwhile, however, many examples of chimera states are known to emerge under a strictly global coupling [18–21]. This is in contrast to the case of 'true' or 'genuine' nearest-neighbor, i.e. local or diffusive, coupling, where chimeras have not been reported yet. With 'true' we indicate here that there is no time-scale separation because it is not possible to adiabatically eliminate fast diffusive degrees of freedom, which constitutes an effective nonlocal spatial coupling [7]. Formation of chimera states under local coupling with time-scale separation in the dynamics was discussed by Laing in [22].

In this article we describe a new, robust mechanism for the emergence of chimera states in a spatially-extended system. Contrarily to all previous works, this mechanism requires no special form of spatial coupling, i.e., it works for strictly local coupling as well and it is thus not linked to any specific interaction function (or, in a wider sense, network topology). Rather, it assumes a local dynamics that requires three variables, the third variable introducing a bistability which allows the coexistence of qualitatively different oscillatory behaviors, among them synchrony and turbulence. The novel mechanism here reported also works as a general model for coexisting dynamical regimes. No-time scale separation is present in the purely local coupling of the *identical* oscillators. We call this a *genuine* local coupling and we demonstrate below the emergence of chimeras under these conditions. Key for the formation of these chimera states are the nonlinearity and the control parameters that set the oscillatory regime close to a supercritical pitchfork–Hopf bifurcation [23]. To observe this bifurcation, in addition to some base oscillator, that needs at least two variables, a third variable is needed that modifies the local properties of the oscillator. Thus, in chemical systems, for example, a minimum of three chemical species is needed (in electrochemical systems, since the double layer potential is also a dynamical variable [24], a minimum of two chemical species would be needed).

The outline of this article is as follows. In Section 2 we present our model and discuss its most prominent features. In Section 3, the uniform solution is described and its stability in parameter plane is established. In Section 4 we show numerical simulations of the model that confirm the intuitions conveyed in Section 3. In Section 5 we establish another important result: a criterion to find chimera states in the parameter plane in our model. Finally, in Section 6 we describe how

* Corresponding author.
E-mail addresses: vladimir.garcia@uv.es (V. García-Morales), jose.a.manzanares@uv.es (J.A. Manzanares), krischer@ph.tum.de (K. Krischer).

https://doi.org/10.1016/j.chaos.2022.112808
Received 29 July 2022; Received in revised form 5 October 2022; Accepted 12 October 2022
Available online 28 October 2022

the model can be used to describe the coexistence of qualitatively different dynamical behaviors which we illustrate with other spatiotemporal patterns.

2. Model

The nonlinear oscillators are modeled by an order parameter $W(x,t) \in \mathbb{C}$ and an internal degree of freedom $\eta(x,t) \in \mathbb{R}$ where x is the position of each oscillator and t time. The order parameter $W = |W|e^{i\varphi}$, with amplitude $|W|$ and phase φ, is the solution of a complex Ginzburg–Landau equation (CGLE) [25–27]. The spatiotemporal evolution of the system is governed by the equations

$$\partial_t W = W + (1 + ic_1)\partial_x^2 W - (1 + ic_2(\eta))|W|^2 W, \tag{1}$$

$$\partial_t \eta = \mu\eta + \partial_x^2 \eta - \eta^3, \tag{2}$$

where

$$c_2(\eta) = a\eta - b \tag{3}$$

and $c_1, \mu, a, b \in \mathbb{R}$ are constants. The combination of a CGLE with an imperfect pitchfork bifurcation has previously been used, with a different coupling between W and η, to describe birhytmic dynamics in a reaction–diffusion system [28,29].

The oscillators are identical because Eqs. (1) and (2) are invariant under the simultaneous translation transformations $W(x,t) \to W(x-d,t)$ and $\eta(x,t) \to \eta(x-d,t)$. The internal variable η is analogous to a locally-averaged magnetic dipole moment of the oscillators. The ensemble behaves, with respect to η, like a 'ferromagnetic substance' in the absence of an externally-applied magnetic field. The value $\mu = 0$ of the control parameter corresponds then to a critical point in a continuous phase transition.

We note that Eq. (1) is coupled to Eq. (2) only through the function $c_2(\eta)$. Eq. (2) is decoupled from Eq. (1) and can be studied separately. The local dynamics of Eq. (2) is given by $\dot{\eta} = \mu\eta - \eta^3$, which is the normal form of a supercritical pitchfork bifurcation. For $\mu < 0$, the unique fixed point $\eta_0^* = 0$ is stable. For $\mu > 0$, the fixed point η_0^* is unstable and there are two stable, symmetry-breaking fixed points $\eta_+^* = \sqrt{\mu}$ and $\eta_-^* = -\sqrt{\mu}$. The spatiotemporal dynamics of Eq. (2), with its diffusion term, is then easily understood. For $\mu < 0$ and any arbitrary initial condition, $\eta(x,t)$ reaches the stationary and spatially-homogeneous profile $\eta^*(x) = \eta_0^*$. For $\mu > 0$, the stationary state reached depends on the initial condition $\eta(x,0)$. On the one hand, both uniform nontrivial steady states (η_+^* or η_-^*) are stable. On the other hand, there is also a wide variety of stable non-uniform profiles consisting of a collection of spatial domains (fronts) whose bulks are, alternatively, in states η_+^* and η_-^* (domains with bulk value η_0^* being absent) separated by an even number of stationary (Ising) walls. We shall call a domain with bulk value η_+^* a *plus-domain* and a domain with bulk value η_-^* a *minus-domain*.

From Eq. (2) the shape of the stationary Ising walls $\eta_{\rm IW}^*(x)$ is given by the solution of $0 = \mu\eta_{\rm IW}^* + \partial_x^2\eta_{\rm IW}^* - (\eta_{\rm IW}^*)^3$. For a wall centered at $x = x_0$ the solutions read $\eta_{\rm IW}^*(x) = \pm\sqrt{\mu}\tanh\left[(x-x_0)\sqrt{\mu/2}\right]$ where the positive sign (resp. negative) describes the wall obtained in passing from a minus-domain to a plus-domain (resp. from a plus-domain to a minus-domain) with increasing x.

In Fig. 1 we illustrate the behavior of Eq. (2) for $\mu > 0$. The initial condition is a pulse of the form $\eta(x,0) = \mathrm{sech}\, x^2 + \xi(x)$ with $\xi(x)$ is a small-amplitude uniform noisy signal. We consider a 1D ring with periodic boundary conditions for simplicity. Then, the order parameter $\eta(x,t)$ evolves to a stationary profile $\eta^*(x)$ formed by one plus and one minus domain separated by Ising walls.

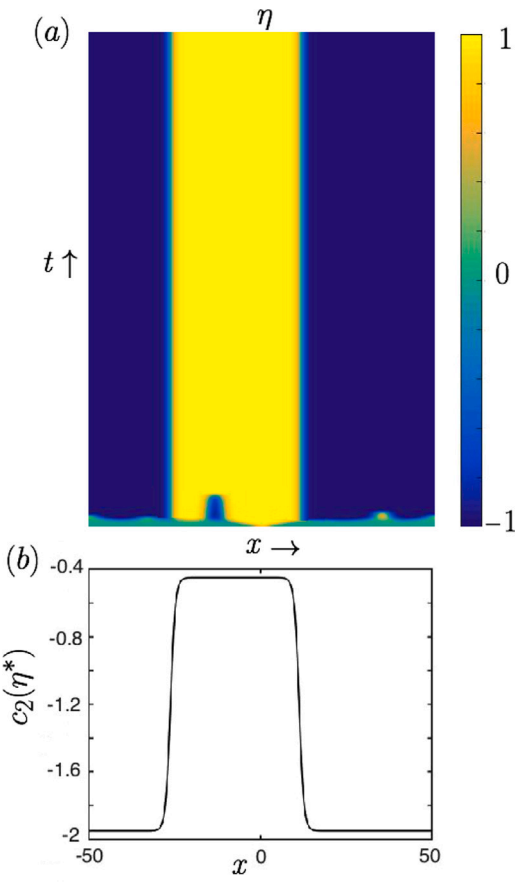

Fig. 1. (a) Spatiotemporal evolution of η (shown are 100 time steps) as provided by Eq. (2) for a ring of size $L = 100$, $\mu = 1$ and a real-valued initial condition consisting of a pulse at $x = 0$ plus added noise; (b) Spatial distribution of c_2 given by Eq. (3) once the stationary spatial profile is reached.

3. The synchronous oscillation and its stability

Let us now evaluate the impact of this behavior in Eq. (1) as the parameter μ is varied in Eq. (2). When $\mu < 0$, since $\eta^*(x) = 0$, after a transient from Eq. (3) we have that $c_2 = -b$ in Eq. (1). We note that, in this regime the uniform, synchronous oscillation of the trivial state

$$W(x,t) = e^{-ic_2 t} = e^{ibt} \tag{4}$$

is a solution of Eq. (1). This synchronous oscillation is linearly stable if

$$c_1 c_2 = -c_1 b > -1 \tag{5}$$

and unstable otherwise. The line $c_1 c_2 = -1$ is the Benjamin–Feir (BF) line, that gives the transition from a stable uniform oscillation to instability in the form of turbulence [25]. If $c_2 = -b$ is fixed and c_1 is increased, a transition from synchrony to turbulence is observed: gradually more Fourier modes become unstable as Eq. (5) is more strongly violated. We thus observe either synchrony or turbulence and no coexistence between the two is possible.

We note that, for $\mu < 0$, at the stationary state of Eq. (2), Eq. (1) has an $\mathbb{S}^1$ symmetry because it is equivariant under a change $W(x,t) \to e^{i\phi}W(x,t)$ (where $\phi \in \mathbb{R}$ is an arbitrary constant). Besides, it has an O(2) symmetry generated by translation invariance $W(x,t) \to W(x-d,t)$ and reflection, $W(x,t) \to W(-x,t)$. The consequence of these symmetries is that spatiotemporal nontrivial solutions of Eq. (1) for $W(x,t)$ live on a two-torus with $\mathbb{S}^1 \times \mathrm{O}(2)$ symmetry.

For $\mu > 0$ the stationary state $\eta^*(x) = \eta_0^* = 0$ of Eq. (2) loses stability and, for suitable perturbations, a continuous stationary profile $\eta^*(x)$

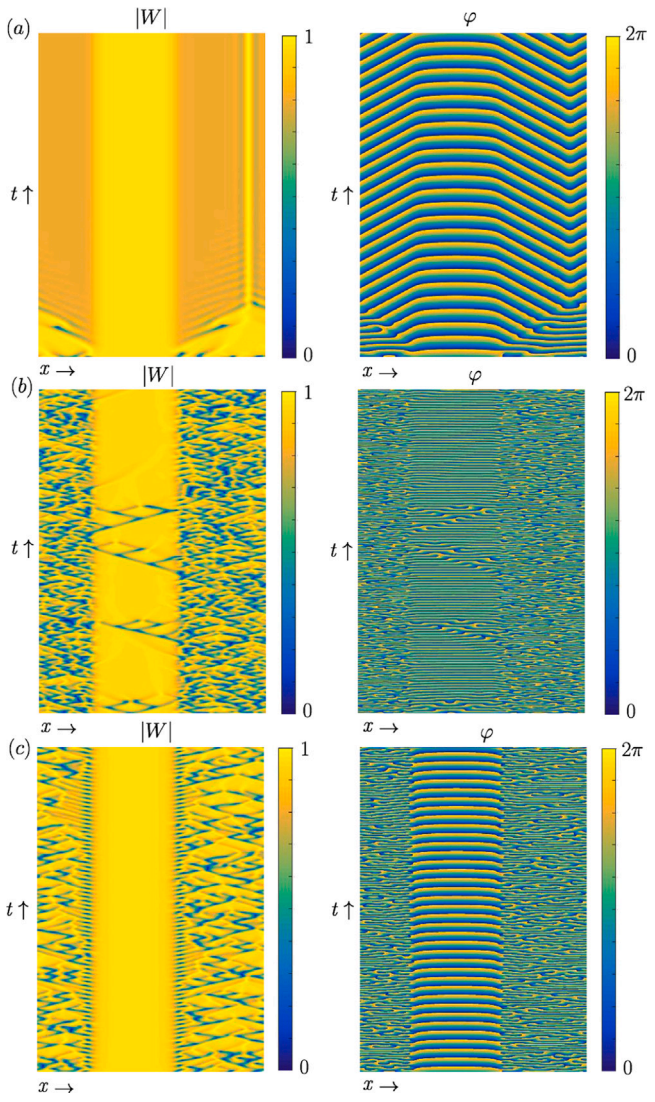

Fig. 2. Spatiotemporal evolution of the absolute value $|W|$ (left panels) and the phase φ (right panels) of the complex order parameter W for $a = 0.2$, $b = 0.5$ (a); $a = 0.75$, $b = 2.25$ (b) and $a = 0.75$, $b = 1.2$ (c). Other parameter values are $\mu = 1$ and $c_1 = 0.7$.

emerges which consists of domains with bulk values $\eta^*_\pm = \pm\sqrt{\mu}$ separated by Ising walls, as described above. Since now, at the stationary state of Eq. (2), $c_2(x) = c_2(\eta^*) = a\eta^*(x) - b$ is spatially dependent, the O(2) symmetry of Eq. (1) is broken. The consequence of this symmetry breaking is that the oscillators arrange into two different kinds of domains (plus and minus-domains) whose qualitative features depend on whether the bulk value is η^*_+ or η^*_-. This O(2) symmetry breaking is the essence behind the separation of the, otherwise identical, oscillators into two distinguished groups. Note that the system of Eqs. (1) and (2) is always O(2) invariant, regardless of the value of μ, but Eq. (1) taken alone is O(2) invariant only for $\mu < 0$, once the stationary state of Eq. (2) is reached.

4. Numerical integration of the model

To better understand the implications of this emergence of different domains, we show in Fig. 2 the spatiotemporal evolution of the absolute value $|W|$ (left panels) and the phase φ (right panels) of the complex order parameter W for $\mu = 1$ and $c_1 = 0.7$ and different choices of the parameters a and b. The initial condition for η is the same as in Fig. 1. The spatiotemporal evolution is obtained by using a spectral

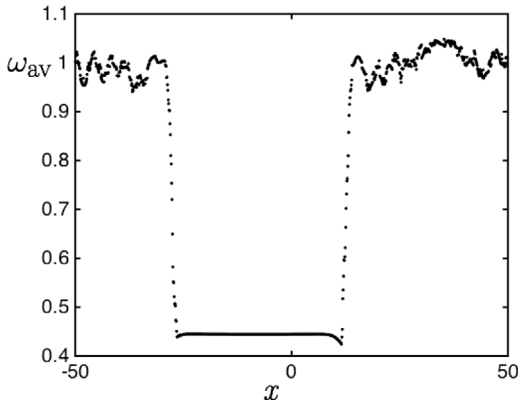

Fig. 3. Average frequency of the oscillators depending on their spatial position x for the chimera pattern of Fig. 2(c).

method with 1024 Fourier modes, periodic boundary conditions and, in Fourier space, the so-called exponential time stepping algorithm ETD2RK described in [30]. In Fig. 2a the parameter values $a = 0.2$, $b = 0.5$ lead to the stationary bulk values $c_2(\eta^*_+) = -0.3$ and $c_2(\eta^*_-) = -0.7$. These bulk values refer to spatial domains with qualitatively different behavior: Since, locally, $c_1c_2 > -1$ for these two bulk values, the homogeneous oscillation is locally stable to long-wavelength perturbations in both domains separately. Besides, other individual Fourier modes can be stable in these domains (depending on their size). This leads to the formation of coherent structures on each of the two phases. In Fig. 2a it is seen that the plus-domain ($x \in [-30, 15]$) displays a homogeneous oscillation while the minus-domain presents a stationary, coherent structure with different spatial periodicity but with the same frequency as the plus domain.

In Fig. 2b the parameter values $a = 0.75$, $b = 2.25$ lead to the stationary bulk values $c_2(\eta^*_+) = -1.5$ and $c_2(\eta^*_-) = -3$. Since now $c_1c_2 < -1$ for either c_2 value, the uniform oscillation is everywhere unstable, the whole ring being in a turbulent regime. However, since $c_2(\eta^*_-) < c_2(\eta^*_+)$, the minus-domain is deeper within the turbulent regime than the plus-domain. This is compellingly reflected by the fact that the average density of phase defects [31] is higher in the minus-domain than in the plus-domain. *Two different turbulent phases coexist spatially in a stable manner*. To the very best of our knowledge, such a spatiotemporal pattern of qualitatively different coexisting turbulent phases has not been reported before.

In Fig. 2c the parameter values $a = 0.75$, $b = 1.2$ lead to the stationary bulk values $c_2(\eta^*_+) = -0.45$ and $c_2(\eta^*_-) = -1.95$. We now have $c_1c_2(\eta^*_+) > -1$ but $c_1c_2(\eta^*_-) < -1$. This means that the homogeneous oscillation is stable in the plus-domain and unstable in the minus-domain. The behavior of the plus-domain is coherent while that of the minus-domain is incoherent. This situation describes a chimera state, as shown in the figure.

In Fig. 3, the average frequency of the oscillators in the chimera state of Fig. 2c is shown. The oscillators within the plus-domain are all phase-locked and oscillate synchronously with the average frequency $\omega_{av} = -c_2(\eta^*_+) = 0.45$ as predicted by Eq. (4). However, the oscillators in the minus-domain are randomly drifting and do not maintain any constant phase difference. These oscillators are in the defect-turbulence regime of the CGLE. Consequently, the average frequency of the oscillators in the minus-domain present noticeable fluctuations for any finite time series both in space and time around a mean value that is about unity. This is half the value $\omega_{av} = -c_2(\eta^*_-) = 1.95$ predicted by Eq. (4). This deviation is not surprising since the homogeneous oscillation is not stable in the minus-domain.

5. A criterion to find chimera states

We thus observe that finding chimera states within our model is aided by a selection of the parameters a and b for fixed $c_1, \mu > 0$ such that the plus-domain satisfies $c_1 c_2(\eta_+^*) = c_1\left(a\sqrt{\mu} - b\right) > -1$ while the minus-domain satisfies $c_1 c_2(\eta_-^*) = c_1\left(-a\sqrt{\mu} - b\right) < -1$. In this way, the plus-domain is coherent and the minus-domain incoherent. These two inequalities can be unified in the following single inequality

$$\left(\frac{1}{c_1} - b\right)^2 - \mu a^2 < 0, \qquad (c_1 > 0) \tag{6}$$

The parameter values for the chimera in Fig. 2c satisfy Eq. (6). The ones in Figs. 2a and 2b do not satisfy it and, therefore, Eq. (6) provides a straightforward guide to find pairs of values such that chimera states arise spontaneously from a large basin of attraction of initial conditions.

Chimera states can thus be directly understood from the CGLE. Indeed, by the methods in [25] (section 3.5), it can be shown that by writing $\varphi := \omega_0 t + \psi$, Eq. (1) can be reduced to the nonlinear phase diffusion equation

$$\partial_t \psi = (1 + c_1 c_2(\eta))\partial_x^2 \psi + \omega_0(c_2(\eta) - c_1)(\partial_x \psi)^2 \tag{7}$$

from which it is observed that when $1 + c_1 c_2(\eta) < 1$, one has a negative phase diffusion coefficient, which implies turbulence and when $1 + c_1 c_2(\eta) > 1$ the phase diffusion coefficient is positive and one has synchrony. Eq. (6) exactly captures these behaviors providing a direct understanding of chimera states from the CGLE and the bistability induced by the internal degree of freedom η. This compellingly shows how, indeed, chimera states are the 'natural link between coherence and incoherence' [32].

6. Coexistence of other spatiotemporal patterns

A knowledge of the phase diagram of the CGLE alone [26] is helpful to design patterns with coexisting domains with qualitatively different dynamical behavior separated by walls. For example, it is known that traveling coherent structures called Bekki–Nozaki holes (BNHs) are obtained from the CGLE for $c_1 = 0$ and $c_2 = 0.5$ [33]. Choosing $a = -1$ and $b = -0.5$ yields $c_2(\eta_-^*) = 0.5$ for the minus-domain and, therefore, it is reasonable to expect that this phase will contain such coherent structures. Since $c_2(\eta_+^*) = -0.5$, the plus-domain will also be composed of coherent oscillators, although the coherent structures found will be similar to those of Fig. 2a. This intuition is confirmed by numerical solution of the CGLE for the initial condition of Fig. 1 and the parameter values $\mu = 1$, $c_1 = 0$, $a = -1$, $b = -0.5$. In Fig. 4 is observed that a BNH is confined to the minus-domain alone while the plus-domain is a standing wave like the one found in the minus-domain of Fig. 2a. The traveling BNH is long lived and is deflected by the walls separating the phases, so that the standing wave in the plus-domain is forever stable and does not interact with the hole solution, which is present only in the minus-domain. This behavior is new but is clearly understood by the role that the supercritical pitchfork bifurcation of Eq. (2) plays in Eq. (1) breaking its O(2) symmetry.

BNHs constitute a one parameter family of traveling localized source solutions which become a subfamily of the dark soliton solutions in the nonlinear Schrödinger limit of the CGLE [34], which corresponds to $c_1 \to \infty$, $c_2 \to \infty$ in the latter. After rescaling of the time variable, the nonlinear Schrödinger equation (NSE) is obtained

$$\partial_t W = \mathrm{i}\frac{c_1}{c_2}\partial_x^2 W - \mathrm{i}|W|^2 W, \tag{8}$$

This NSE, and modifications of it including different potentials and/or fractional dynamics, are of major importance in the study of wave propagation in optical fibers [35,36] and soliton solutions [37–39], for which there exists a vast literature (some recent relevant works are [40–45]). Usually, to describe the co-propagation behavior of two or more optical pulses in phase modulation systems, several NSEs are coupled [42] and higher dimensions are also considered, for example in bullet-like solitons in three-dimensions [41]. We note that the NSE can be obtained from our system of Eqs. (1) to (3) by taking $c_1 \to \infty$, $a \to \infty$ and $b \to -\infty$ while keeping the quotient $c_1/c_2(\eta)$ finite. If one or more such NSEs are coupled to Eq. (2), one can envisage spatially confining the solitons to certain regions created by the bistable dynamics of the internal degree of freedom η although further research is necessary to confirm this expectation. The general phase separation mechanism here introduced can, indeed, be extended by coupling any nonlinear partial differential equation (PDE) (or system of them) to Eq. (2) so that the internal degree of freedom η produces the separation of different phases present in the bifurcation diagram of the corresponding nonlinear PDE(s). Therefore, instead of the CGLE, other pattern-forming nonlinear PDEs [46], such as the Korteweg–de Vries equation [37,47], the Kadomtsev–Petviashvili (KP) equation [48,49] or the Burgers system [50,51] can be investigated as well.

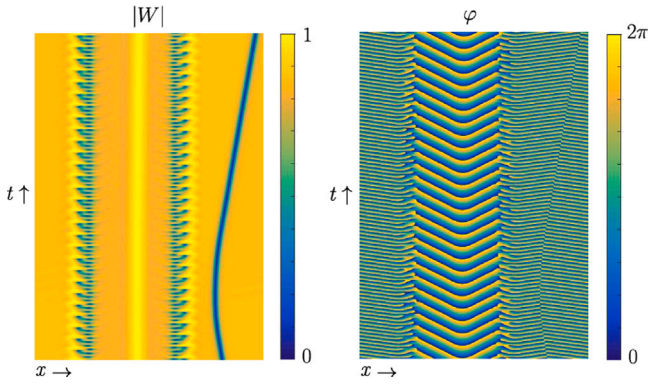

Fig. 4. Spatiotemporal evolution of the absolute value $|W|$ (left) and the phase φ (right) of the complex order parameter W for $a = -1$, $b = -0.5$, $\mu = 1$ and $c_1 = 0$.

7. Conclusions

In this article, a new mechanism for the emergence of chimera states has been described and the location of these states in parameter plane has been established. Furthermore, a mechanism for phase separation in a system governed by nonlinear PDEs has been sketched and illustrated by bringing into coexistence different qualitative behaviors of the CGLE. The model is minimalistic and captures the essence of the formation of domains with qualitatively different dynamical behavior. The coupling of the identical oscillators is genuinely local, meaning that, being purely diffusive, it is such that no time-scale separation is present in the degrees of freedom of the system. Nonlocal [7] and global [19] modifications of the complex Ginzburg–Landau equation (CGLE) were previously introduced to describe chimera states. In this work, we have shown that the CGLE together with a bistable, internal degree of freedom, provides an alternative, 'natural' mechanism to chimera states. Robust chimeras arise spontaneously in wide parameter regimes with a large basin of attraction.

CRediT authorship contribution statement

Vladimir García-Morales: Conceptualization, Methodology, Analysis and/or interpretation of data, Validation, Formal analysis, Writing – original draft, Visualization, Investigation, Writing – review & editing. **José A. Manzanares:** Conceptualization, Methodology, Analysis and/or interpretation of data, Formal analysis, Writing – original draft, Investigation, Writing – review & editing. **Katharina Krischer:** Conceptualization, Methodology, Analysis and/or interpretation of data, Formal analysis, Writing – original draft, Investigation, Writing – review & editing.

Declaration of competing interest

The authors declare that they have no known competing financial interests or personal relationships that could have appeared to influence the work reported in this paper.

Data availability

Data will be made available on request.

References

[1] Panaggio MJ, Abrams DM. Nonlinearity 2015;28:R67.
[2] Schöll E. Eur Phys J Spec Top 2016;225:891.
[3] Omel'chenko OE. Nonlinearity 2018;31:R121.
[4] Parastesh F, Jafari S, Azarnoush H, Shahriari Z, Wang Z, Bocaletti S, et al. Phys Rep 2020;898:1.
[5] Haugland S. J Phys Complex 2021;2:032001.
[6] Abrams DM, Strogatz SH. Phys Rev Lett 2004;93:174102.
[7] Kuramoto Y, Battogtokh D. Nonlinear Phenom Complex Syst 2002;5:380.
[8] Shima SI, Kuramoto Y. Phys Rev E 2004;69:036213.
[9] Masoliver M, Davidsen J, Nicola W. Commun Phys 2022;5:205.
[10] Wang Z, Liu Z. Front Physiol 2020;11:724.
[11] Andrzejak RG, Rummel C, Mormann F, Schindler K. Sci Rep 2016;6:23000.
[12] Lainscsek C, Rungratsameetaweemana N, Cash SS, Sejnowski TJ. Chaos 2019;29:121106.
[13] Tinsley MR, Nkomo S, Showalter K. Nat Phys 2012;8:662.
[14] Hagerstrom AM, Murphy TE, Roy R, Hövel P, Omelchenko I, Schöll E. Nat Phys 2012;8:658.
[15] Nkomo S, Tinsley MR, Showalter K. Phys Rev Lett 2013;110:244102.
[16] García-Morales V. Europhys Lett 2016;114:18002.
[17] García-Morales V. Commun Nonlinear Sci Numer Simul 2018;63:117.
[18] Sethia GC, Sen A. Phys Rev Lett 2014;112:144101.
[19] Schmidt L, Schönleber K, Krischer K, García-Morales V. Chaos 2014;24:013102.
[20] Kaneko K. Chaos 2015;25:097608.
[21] Yeldesbay A, Pikovsky A, Rosenblum M. Phys Rev Lett 2014;112:144103.
[22] Laing CR. Phys Rev E 2015;92. 050904(R).
[23] Kuznetsov YI. Elements of applied bifurcation theory. 3rd ed.. New York: Springer; 2004, p. 286–7.
[24] Krischer K. In: Alkire RC, Kolb DM, editors. Advances in electrochemical sciences and engineering. Weinheim: Wiley-VCH; 2003, p. 89–208.
[25] Kuramoto Y. Chemical oscillations, waves and turbulence. Berlín: Springer; 1984.
[26] Aranson IS, Kramer L. Rev Modern Phys 2002;74:99.
[27] García-Morales V, Krischer K. Contemp Phys 2012;53:79.
[28] Stich M, Ipsen M, Mikhailov AS. Phys Rev Lett 2001;86:4406.
[29] Stich M, Ipsen M, Mikhailov AS. Physica D 2002;171:19.
[30] Cox SM, Matthews PC. J Comput Phys 2002;176:430.
[31] Shraiman BI, Pumir A, van Saarloos W, Hohenberg PC, Chaté H, Holen M. Physica D 1992;57:241.
[32] Omel'chenko OE, Maistrenko YL, Tass PA. Phys Rev Lett 2008;100:044105.
[33] Burguete J, Chaté H, Daviaud F, Mukolobwiez N. Phys Rev Lett 1999;82:3252.
[34] Stiller O, Popp S, Aranson I, Kramer L. Physica D 1995;87:361.
[35] Gao X-Y, Guo Y-J, Shan W-R. Appl Math Lett 2021;120:107161.
[36] Yang D-Y, Tian B, Qu Q-X, Zhang C-R, Chen S-S, Wei C-C. Chaos Sol Fract 2021;150:110487.
[37] Toda M. Nonlinear waves and solitons. Mathematics and its applications (Japanese series), Tokyo: KTK Scientific Publishers; 1989.
[38] Drazin PG, Johnson RS. Solitons: an introduction. Cambridge, UK: Cambridge University Press.; 1990.
[39] Dauxois T, Peyrard M. Physics of solitons. Cambridge, UK: Cambridge University Press; 2006.
[40] Shen Y, Tian B. Appl Math Lett 2021;122:107301.
[41] Wen X-K, Feng R, Lin J, Liu W, Chen F, Yang Q. Optik 2021;248:168092.
[42] Fang Y, Wu G-Z, Wen X-K, Wang Y-Y, Dai C-Q. Opt Laser Technol 2022;155:108428.
[43] Wen G-Z, Wu X-K, Liu W, Dai C-Q. Nonlinear Dyn 2022;109:3041.
[44] Belyaeva TL, Agüero MA, Serkin VN. Optik 2021;244:167584.
[45] Cao Q-H, Dai C-Q. Chin Phys Lett 2021;38:090501.
[46] Cross MC, Hohenberg PC. Rev Modern Phys 1993;65:851.
[47] Gao X-Y, Guo Y-J, Shan W-R. Commun Theor Phys 2020;72:095002.
[48] Ablowitz MJ, Segur H. Solitons and the inverse scattering transform. Philadelphia, PA: SIAM; 1981.
[49] Gao X-Y, Guo Y-J, Shan W-R. Chin J Phys 2022;77:2707.
[50] Gao X-Y, Guo Y-J, Shan W-R. Chaos Sol Fract 2022;161:112293.
[51] Zhou T-Y, Tian B, Chen Y-Q, Shen Y. Nonlinear Dynam 2022;108:2417.